Supplement of
High emission rates and strong temperature response make boreal wetlands a large source of isoprene and terpenes

Lejish Vettikkat[1], Pasi Miettinen[1], Angela Buchholz[1], Pekka Rantala[2], Hao Yu[3], Simon Schallhart[4], Tuukka Petäjä[2], Roger Seco[5], Elisa Männistö[6], Markku Kulmala[2], Eeva-Stiina Tuittila[6], Alex B. Guenther[7] and Siegfried Schobesberger[1]

[1]Department of Applied Physics, University of Eastern Finland, Kuopio, P.O. Box 1627, FI-70211, Finland
[2]Institute for Atmospheric and Earth System Research, University of Helsinki, Helsinki, 00014, Finland
[3]Department of Environmental and Biological Sciences, University of Eastern Finland, Kuopio, P.O. Box 1627, FI-70211, Finland
[4]Finnish Meteorological Institute, P.O.Box 503, FI-00101 Helsinki, Finland
[5]Institute of Environmental Assessment and Water Research (IDAEA-CSIC), 08034 Barcelona, Catalonia, Spain
[6]Peatland and soil ecology research group, School of Forest Sciences, University of Eastern Finland, P.O. Box 111, 80101 Joensuu, Finland
[7]Department of Earth System Science, University of California, Irvine, Irvine, California, USA

Correspondence to: Lejish Vettikkat (lejivett@uef.fi) and Siegfried Schobesberger (siegfried.schobesberger@uef.fi)

Table S1. Portions of five different vegetation community types and their mean total moss cover (%) in the 90 % flux contribution in the footprint area of the VOC measurements in Siikaneva I.

Vegetation community type	LAI shrub	LAI other	% of the footprint	mean moss %
Carex lasiocarpa lawn	0.003	0.005	2	94.1
Carex rostrata lawn	0.044	0.066	32	96.9
Eriophorum vaginatum lawn	0.073	0.102	47	95.4
Wet hollow	0.005	0.033	11	93.7
Dry hummock	0.024	0.031	8	94.0
Total	**0.15**	**0.24**	**100**	**95.5**

Table S2. The measured monoterpenes and their amount in the adsorbent tubes (in ng).

Monoterpene	Wooden platform (ng)	close to the wetland (ng)	Top of Vocus-PTR (ng)
α-pinene	4.72	2.60	1.30
camphene	0.52	0.73	0.63
β-pinene	0.73	0.71	0.18
3-carene	3.60	1.23	0.57
limonene	0.52	0.36	0.22

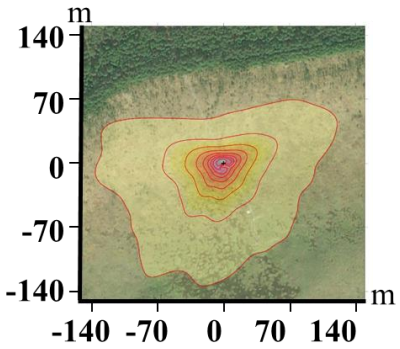

Figure S1. Map of the Siikaneva fen site with average two-dimensional footprint for the whole campaign for periods yielding quality-controlled fluxes (details in SI). The contours represent the footprint at flux contribution intervals of 10 to 90% in 10% steps. The base map image is taken from ©Google Maps.

S1 Data analysis

S1.1 Vocus-PTR Calibrations

Regular calibrations (n=13) were performed throughout the campaign using the inbuilt calibration system, except for occasions when the calibration gas canister was empty or during power failures, or when the ToF power supply (TPS) connection was lost (n=27). The four-point calibration provided mixing ratios of 0, 2.5, 5, and 10 ppbv using a gas standard (Apel Riemer Environmental Inc.) containing 15 VOCs (including isoprene and α-pinene) of known mixing ratio (~1 ppm for each component). The calibration gas was dynamically diluted using clean air from a zero-air generator (Aerodyne Inc. USA). This "zero-air" was also used to perform continuous automated background determinations ("zeros") for 15 seconds every 15 minutes throughout the campaign. The sensitivity of the Vocus-PTR to different VOCs is linearly related to their respective proton transfer rate constants (k_{ptr}) after transmission, and fragmentation of these VOCs inside the instrument is considered (Krechmer et al., 2018). Using the derived sensitivities for acetone (observed

as $C_3H_7O^+$), isoprene ($C_5H_9^+$), benzene ($C_6H_7^+$), toluene ($C_7H_{10}^+$), and methyl ethyl ketone ($C_4H_9O^+$) from calibrations, and literature knowledge of their respective proton transfer rate constants (k_{ptr}), we performed linear regressions to obtain an empirical relationship between the sensitivities and k_{ptr}. Figure S2 shows the measured sensitivities (cps/ppbv) vs. k_{ptr} for each calibration measurement. Empirical relations in the range of:

$$\text{Sensitivity (cps/ppbv)} = 4.7\text{-}8.2 \cdot 10^{11} \cdot k_{ptr} \ (R^2>0.8)$$

were obtained from each calibration. Figure S3 shows the time series of isoprene and α-pinene sensitivities throughout the campaign. The average sensitivities for all the 13 calibrations were 323±73 cps/ppbv for isoprene and 329±83 cps/ppbv for α-pinene (m/z 137.13).

These sensitivities were much lower than those obtained with the same instrument in measurement campaigns before and after our campaign. A measurement campaign in July 2020 reported 880 cps/ppbv for isoprene and 982 cps/ppbv for α-pinene. Another study in October 2021 obtained 682 cps/ppbv for isoprene and 1094 cps/ppbv for α-pinene. However, the instrumental background siloxanes were detected with very similar sensitivity and behaved similarly with temperature variations before, after, and during our campaign. This suggests that the instrument performance did not change significantly but that a leak in the calibration gas delivery line to the capillary inlet occurred during our calibrations, i.e., less of the calibration gas was sampled than assumed, leading to apparently lower sensitivities. Assuming that this leakage led to a constant bias in our calibrations, we calculate the factor that our calibrations differ from the one before and after our campaign. A factor of 2.41 for isoprene and 3.16 for α-pinene were obtained and then used to scale each of our calibration measurements. The so-scaled sensitivity values were linearly interpolated between the calibration measurements to calculate the mixing ratios of the terpenes. The average corrected sensitivity for all the 13 calibrations was 775 cps/ppbv for isoprene and 1040 cps/ppbv for α-pinene (m/z 137.13).

The calibration gas only contained α-pinene as a proxy for monoterpenes (MTs), while the measured MT emissions were a mixture of α-pinene, 3-carene, β-pinene, camphene, limonene, and others (detected by GC-MS analysis). The fragmentation pattern of the measured MTs and α-pinene in the calibration gas mix looked similar during most of our campaign. Therefore, we generically applied the sensitivity for α-pinene to the count rates of $C_{10}H_{17}^+$. Being unable to differentiate between monoterpene isomers will cause only minor uncertainties since the k_{ptr} values of most monoterpenes lie within a narrow range of 2.44 - 2.63 $\times 10^{-9}$ molecule cm^3 s^{-1} (Zhao and Zhang, 2004). Since there were no sesquiterpenes or diterpenes in the calibration gas standard and we are uncertain about their fragmentation pattern, the sensitivities for these compounds were estimated based on the α-pinene sensitivity assuming α-pinene fragmentation in the Vocus-PTR is similar to that of SQTs and diterpenes. We acknowledge that the fragmentation patterns can differ for MT and SQT (Kari et al., 2018). Sesquiterpenes have a higher k_{ptr} of 3.0×10^{-9} molecule cm^3 s^{-1} (Dhooghe et al., 2008) than monoterpenes with a k_{ptr} of 2.5×10^{-9} molecule cm^3 s^{-1} (Zhao and Zhang, 2004). Hence, we used a factor of 1.2 and multiplied it by the measured α-pinene sensitivity to get the SQT sensitivity (Kim et al., 2009). There is no published proton transfer reaction rate for diterpenes; hence, only an upper limit for sensitivity was assigned. We observed the highest sensitivity for the MEK present in our calibration standard, and therefore, we used it as a measure for the maximum expected sensitivity for unknown compounds. Therefore, we used a factor of 1.3 calculated using k_{ptr} of MEK (3.21×10^{-9} molecule cm^3 s^{-1}) and multiplied it by the measured monoterpene sensitivity to get the sensitivity for diterpenes. Since the diterpene sensitivity was estimated based on the α-pinene fragmentation and assuming an upper limit for sensitivity, our diterpene mixing ratios and fluxes may represent lower limits.

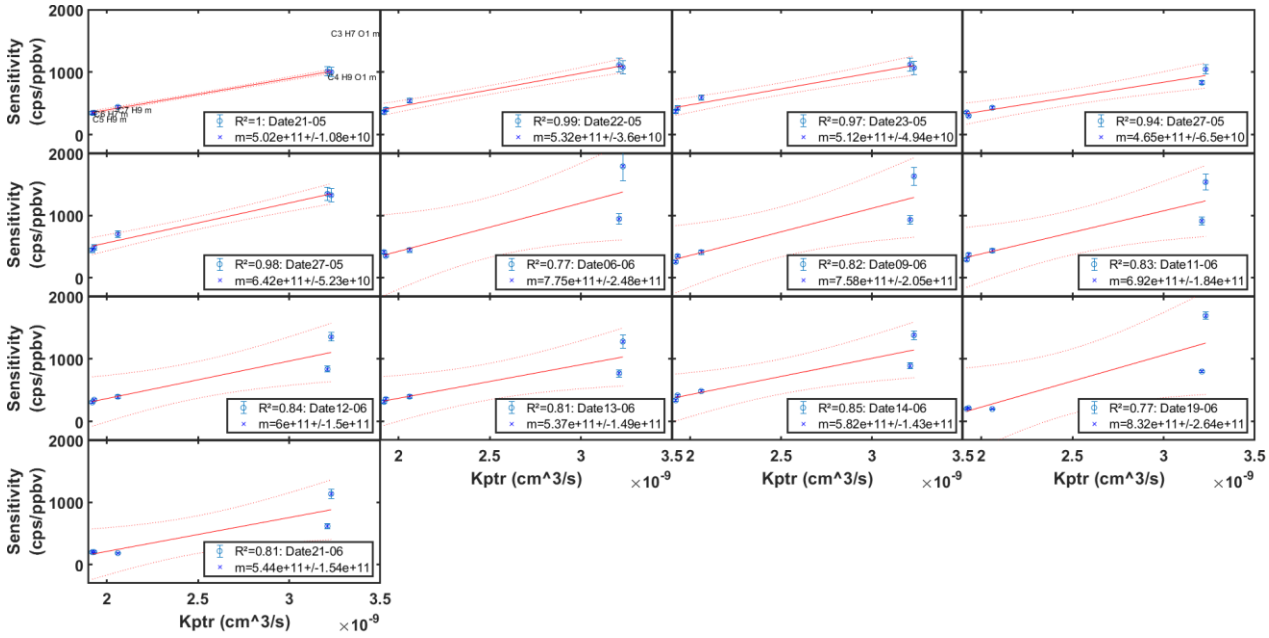

Figure S2. Measured sensitivities (cps/ppbv) vs. k_{ptr} of acetone, isoprene, benzene, toluene, and methyl ethyl ketone. The empirical linear relationship is valid for all 13 calibrations ($R^2 > 0.75$).

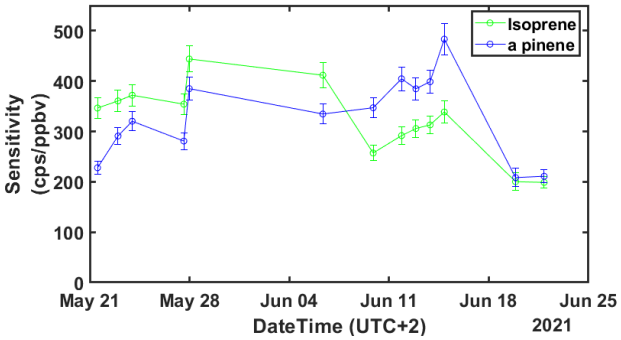

Figure S3. Timeseries of measured sensitivities (cps/ppbv) of isoprene and α-pinene. The error bars show the uncertainty (±σ) resulting from the uncertainties of the VOC calibration standard mixing ratio, mass flow controllers used for dilution, and drifts in instrument response during each calibration.

S1.2 Pre-processing

The high-time resolution time-of-flight data was recorded using the TofDaqRec software in HDF5 format and took up about 40 GB d^{-1}. A MATLAB-based software package, tofTools R611(Junninen et al., 2010), was used to pre-process these raw data files. The spectra were mass calibrated every 5 seconds using suitable peaks up to m/z 371. The peak shape and peak identification were conducted with 1-minute averaged files and then used to fit the 10 Hz data. We identified 1072 elemental compositions in the mass spectra. A high-performance LINUX-based server (48 core CPU) and the MATLAB parallel computing toolbox were utilized for fast, high-resolution peak fitting. It took about 1h to fit all 1072 peaks for 1 day of 10 Hz data. The instrument background was removed by interpolating the regular zero measurements and subtracting from the measured signal for each peak. The calibration-based sensitivity factors were applied to get the mixing ratios of the terpenes.

S1.3 EC flux calculations

The eddy covariance fluxes were calculated using the innFLUX code by Striednig et al. (2020). The innFLUX routine performs a directional planar fit for tilt correction of the wind data. It calculates the covariance between the linearly detrended VOC mixing ratio and tilt corrected vertical component of the wind vector for each 30-minute time interval. We chose a time interval of 30 minutes to calculate the flux, which resulted in good stationarity while reducing low-frequency attenuation. The innFLUX code also follows standard EC procedures such as lag time determination and calculates quality classes for each time interval based on the integral turbulence characteristics (ITC) test and the stationarity test for each compound (Foken et al., 2004). The onward analyses are performed only using data from quality classes 1-3 and with friction velocity > 0.1 m/s. Table S2 shows the class determination criteria used for quality control of the fluxes. The cumulative covariance was used to determine reliable lag times for low signal-to-noise ratio data, and the flux was recalculated using this lag time. We observed a lag time of 0.1-0.2s for the cumulated covariance for all terpenes.

Table S3. Quality control tests and class determination look-up table. (Adapted from (Foken et al., 2004)). For the stationarity test, the range refers to the relative difference between the covariance of each subinterval (typically six subintervals of 5 min for a 30 min time interval) to the 30 min covariance. For the ITC test, the range is the ratio of the standard deviation of the fluctuating parameter to the corresponding dynamical parameter with a model by Foken and Wichura (1996). The stationarity test is given slightly more weight than the ITC test to determine the overall quality criteria.

Stationarity test		**Integral turbulence Characteristics (ITC)**		**Stationarity test**	**ITC test**	**Overall quality**
class	**Range**	**class**	**Range**	**class**	**class**	**class**
1	0–15 %	1	0–15 %	1	1-2	1
2	16–30 %	2	16–30 %	2	1-2	2
3	31–50 %	3	31–50 %	1-2	3-4	3
4	51–75 %	4	51–75 %	3-4	1-2	4
5	76–100 %	5	76–100 %	1-4	3-5	5
6	101–250 %	6	101–250 %	5	≤5	6
7	251–500 %	7	251–500 %	≤6	≤6	7
8	501–1000 %	8	501–1000 %	≤8	≤8	8
9	> 1000 %	9	> 1000 %	9	9	9

S1.4 Co-spectral analysis

The co-spectral analysis is used to assess the frequencies (inversely relating to the size of the eddies) that contribute to the covariance of two variables. We used the empirical method of referring to the co-spectra of temperature, assumed to be unattenuated, to correct for the attenuation of terpene fluxes. Co-spectra were calculated using the recalculated lag times to ensure that the analysis was not affected by low-quality data. Only the daytime co-spectra that passed the quality criteria were averaged and normalized to the mean flux. Figure S4(a) shows these average normalized co-spectra of the

terpenes and temperature throughout the campaign. A power dependence on frequency (f) of $f^{-4/3}$ is obtained for the high-frequency part of the temperature flux (or sensible heat flux) co-spectra, as theoretically expected for the inertial subrange (Kaimal et al., 1972). This co-spectrum was used to calculate the response time and to construct a transfer function for each of the terpenes following the Horst (1997) approach. Figure S4(b) shows each terpene's respective transfer functions and response times. Figure S4(c) shows the correction factor (F_{corr}) estimated using the method proposed by Fratini et al. (2012). We only used the T co-spectrum in calculating F_{corr}. when the value of w´T´ exceeded 0.02 mºC We estimate a high-frequency flux attenuation of 27% for isoprene, 28% for MT, and 29% for SQT. This dampening was not due to interactions of terpenes with surfaces since the high-frequency attenuation was similar for all terpenes. We suspect that the large sampling volume close to the ground might dampen the high-frequency eddies. Since the dampening was similar for all terpenes and due to high noise in diterpenes co-spectra, we used the SQTs response time and correction factor to correct the high-frequency flux attenuation of diterpenes.

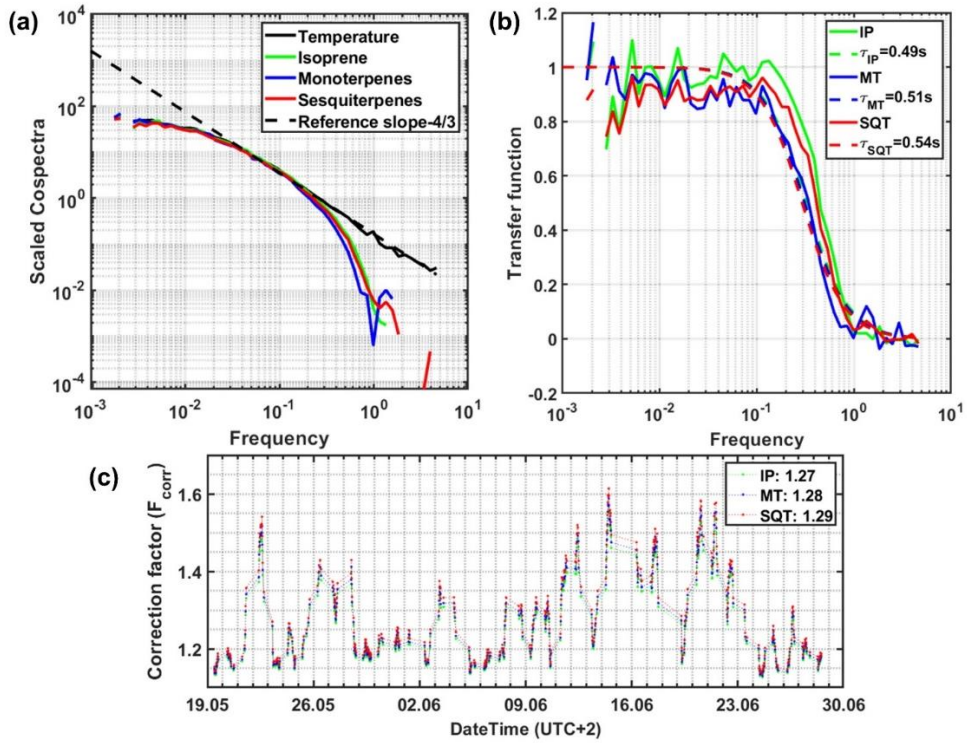

Figure S4 a) Averaged scaled co-spectra of temperature and terpenes. IP is isoprene, MT is monoterpenes, and SQT is sesquiterpenes. Also shown, for reference, is the slope corresponding to the $f^{-4/3}$ power law (dashed line), as expected for high frequencies. b) Transfer function with response times for the terpenes. c) Correction factors (F_{corr}) of half-hourly terpene fluxes calculated with response times from the transfer function. The values in the inset are average over the whole campaign.

S1.5 Uncertainties

The main quantifiable uncertainty was the uncertainty of the Vocus-PTR sensitivity during calibrations. For the terpenes in the calibration mixture, namely, isoprene and monoterpenes, we calculated a total calibration uncertainty using the uncertainties of the VOC calibration standard mixing ratio, mass flow controllers used for dilution, and the drift of the instrument response during each calibration. For isoprene, this uncertainty in sensitivity ranged from 5.7-8.7%, with a mean value of 6%. It ranged from 5.8-6.3% for monoterpenes, with a mean of 6%. For the 13 calibrations performed throughout the campaign, the standard error of measurement of sensitivities was 6.3% for isoprene and 7% for

monoterpenes. Hence the total sensitivity uncertainty was 8.7% for isoprene and 9.2% for monoterpenes. We estimated SQTs sensitivity from monoterpene sensitivity using theoretical proton transfer reaction rates with an uncertainty of 10% (Dhooghe et al., 2008). Considering this uncertainty, we estimate the total uncertainty in sensitivity for SQTs to be 17%. The diterpenes sensitivity was estimated from monoterpenes sensitivity assuming an upper limit for sensitivity, and we assume this assumption to cause uncertainty of 30%.

Another random uncertainty lies in determining the factor to correct the high-frequency flux attenuation. We estimated uncertainty in the correction factor of 11.4% for isoprene, 11 % for MT, and 10.3% for SQT from the uncertainty of the fit parameters for the fit shown in Fig S4a. Since the F_{corr} was 27-29%, this accounts for the uncertainty of about 3 % towards the flux. Since the transfer function of diterpenes was noisy, we used the same F_{corr} used for SQTs to correct the high-frequency flux attenuation of diterpenes. Random uncertainties in the flux of the terpenes were computed using the innFLUX routine. We used the random flux level estimation by random shuffle criteria (Billesbach, 2011). We obtained an uncertainty of 4.5 % for isoprene, 8.3% for MT, 7.4% for SQTS, and 3.9% for diterpenes. From these three random uncertainties, the total random uncertainties were calculated to be 10.3% for isoprene, 12.8% for MT, and 18.8% for SQT. If we assume the uncertainty in the sensitivity calibration of diterpenes to be 30%, the total random uncertainty is 31.1%. In addition, there are two more potentially significant sources of uncertainty, which we did not quantify. Since we determined lower sensitivities for Vocus-PTR overall than in the campaigns before and after, we suspected a leak in the calibration gas delivery line to the capillary inlet (see section S1.1). We used a correction factor based on the calibrations done before and after our campaign to correct our sensitivities (see section S1.1). We also implicitly assumed that the fragmentation of all MT, SQT, and diterpenes in the FIMR of the Vocus-PTR was similar to α-pinene. Neither of these two uncertainties was accounted for in this study and may increase the uncertainty drastically.

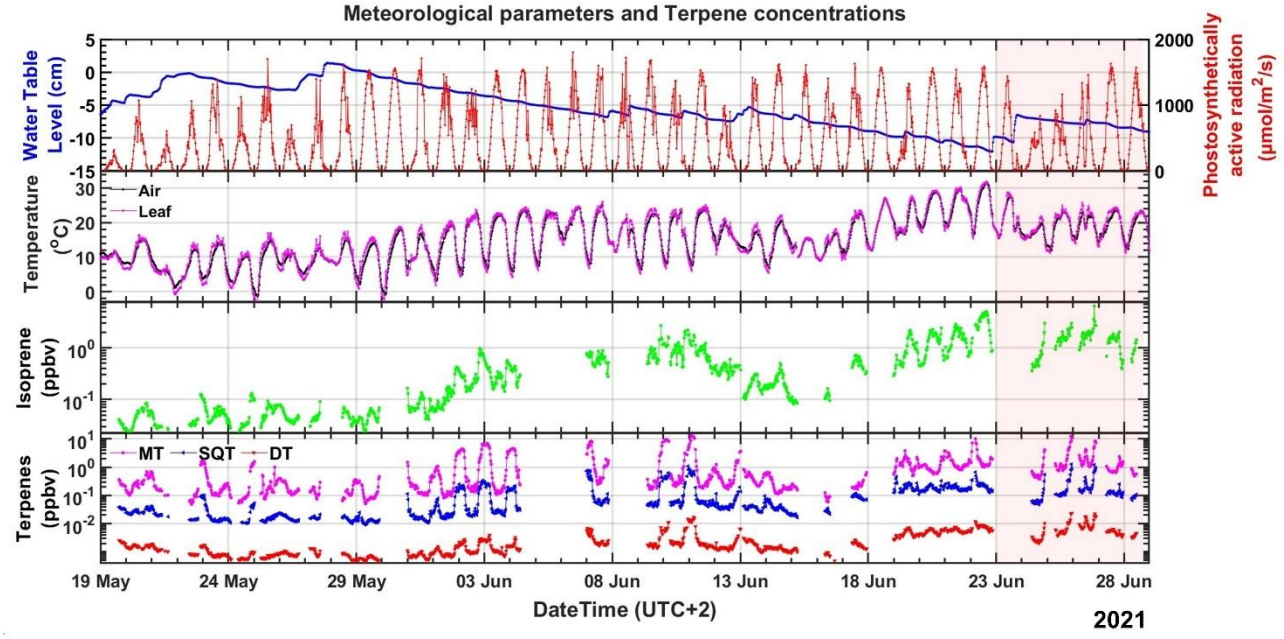

Figure S5. Meteorological parameters and measured terpene concentrations throughout the field campaign at the Siikaneva 1 boreal fen site. The period with red background color after 22 June 2022, the highest temperature day, is referred to as the "high-temperature stress period".

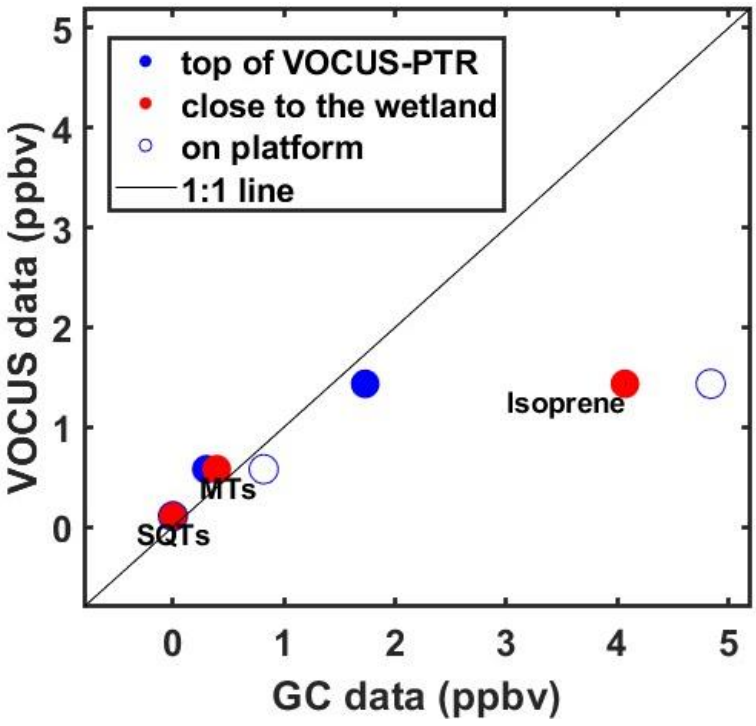

Figure S6. Terpene mixing ratios measured using Vocus-PTR and GC-MS from 11:30 to 12:00 on 28 June 2021. The GC adsorbent tubes were collected at different locations (close to the wetland, on top of the Vocus-PTR, and near the wooden platform). The solid black line is the 1:1 line to guide the eye.

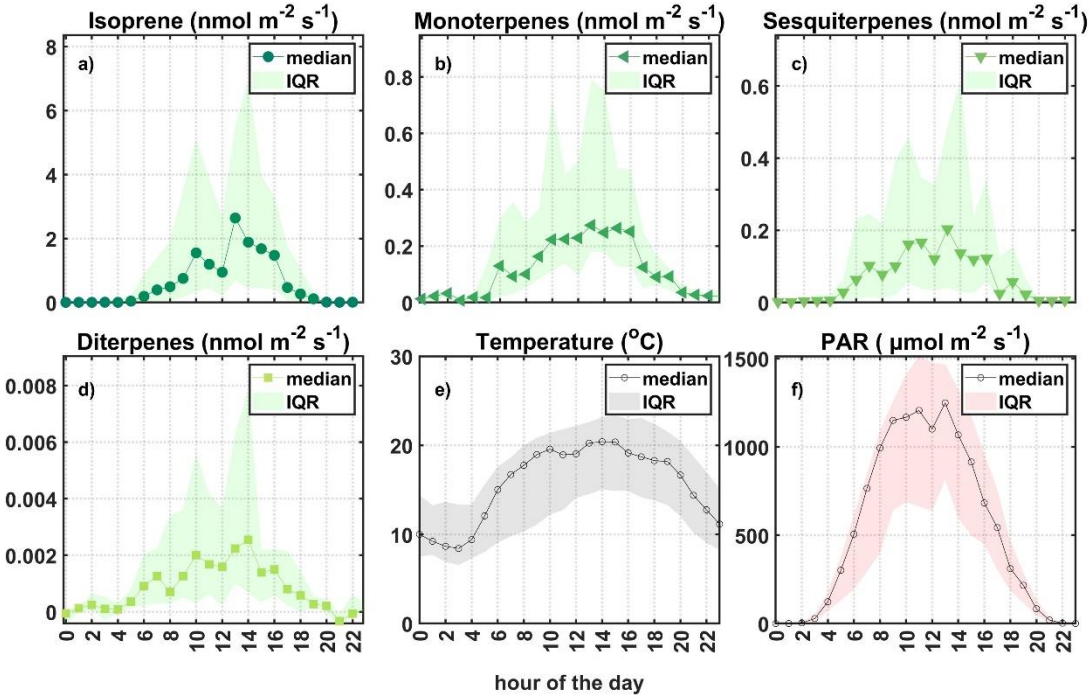

Figure S7. Diurnal cycle of fluxes of the terpenes, PAR, and T. Shaded areas indicate the interquartile range (IQR).

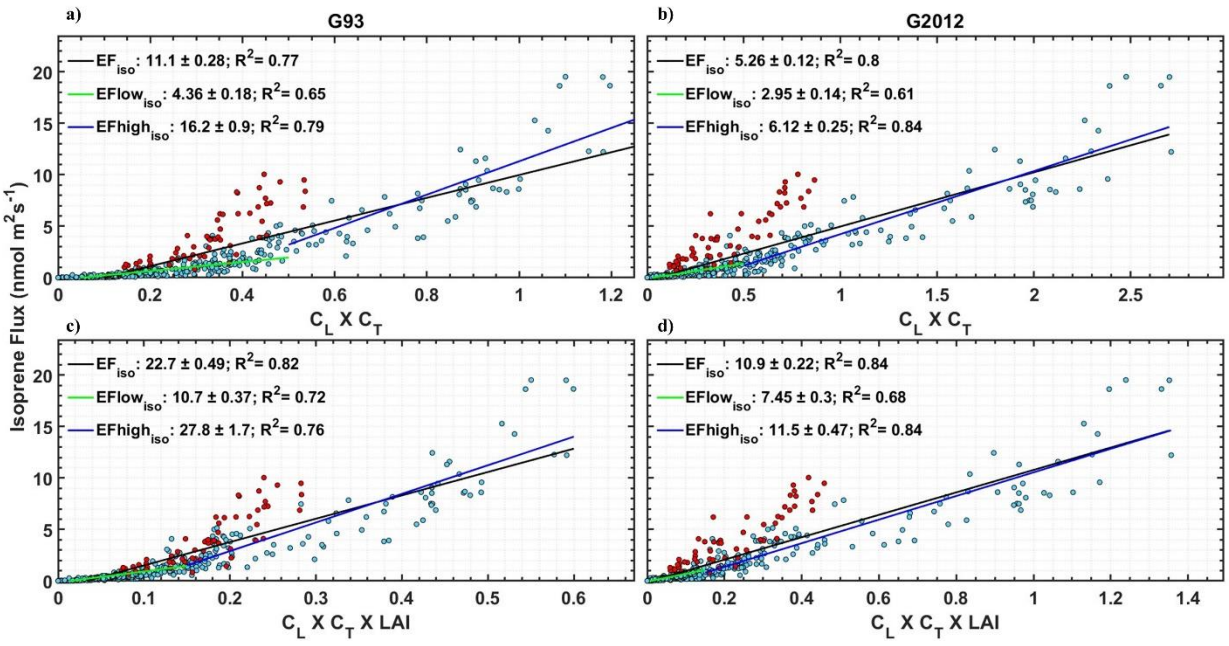

Figure S8. Isoprene fluxes plotted vs. the combined light (C_L) and temperature (C_T) activity factors (C_L x C_T) factors (panels a-b) and C_L x C_T x LAI (panels c-d), respectively, as used in G93 (left panels) and G2012 (right panels). As per Eq. 1, the linear regression slope gives the isoprene emission factor at the standardized conditions for the fen (EF_{iso}, T=30 °C, PAR=1000 µmol m^{-2} s-1, and LAI =1). The red data points are the flux measurements during the "high-temperature stress period" and are included in the fits and hence EF determinations. The green slope gives EF for the lower half ($EFlow_{iso}$: C_L x C_T < 0.5), and the blue slope gives the EF for the higher half ($EFhigh_{iso}$: C_L x C_T > 0.5).

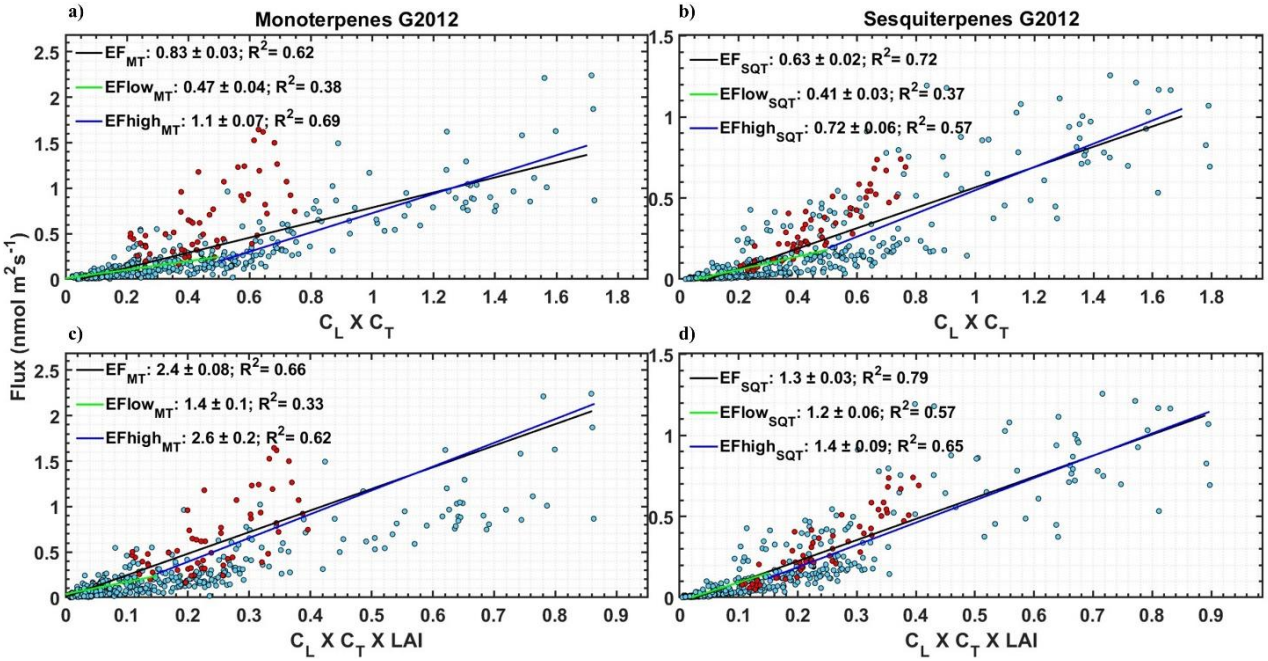

Figure S9. Emission fluxes combined C_L x C_T factors and C_L x C_T x LAI respectively of the monoterpenes (a and c) and sesquiterpenes (b and d) using G2012 algorithms (Guenther et al. 2012.) The linear regression slope gives the emission factor at standard conditions for the fen (EF_{MT}, EF_{SQT}, T=30 C, PAR=1000 µmol m^{-2} $s^{-1,}$ and LAI =1). The red data points are the flux measurements during the "high-temperature stress period" and are included in the EF calculations. The green slope gives EF for the lower half ($EFlow_{iso}$: C_L x C_T < 0.5), and the blue slope gives the EF for the higher half ($EFhigh_{iso}$: C_L x C_T > 0.5).

2 References

Billesbach, D.: Estimating uncertainties in individual eddy covariance flux measurements: A comparison of methods and a proposed new method, Agricultural Forest Meteorology, 151, 394-405, 2011.

Dhooghe, F., Amelynck, C., Schoon, N., Debie, E., Bultinck, P., and Vanhaecke, F.: A selected ion flow tube study of the reactions of H3O+, NO+ and O2+ with a series of sesquiterpenes, International Journal of Mass Spectrometry, 272, 137-148, 2008.

Foken, T. and Wichura, B.: Tools for quality assessment of surface-based flux measurements, 78, 83-105, 1996.

Foken, T., Göockede, M., Mauder, M., Mahrt, L., Amiro, B., and Munger, W.: Post-field data quality control, in: Handbook of micrometeorology, Springer, 181-208, 2004.

Fratini, G., Ibrom, A., Arriga, N., Burba, G., and Papale, D.: Relative humidity effects on water vapour fluxes measured with closed-path eddy-covariance systems with short sampling lines, Agricultural and Forest Meteorology, 165, 53-63, https://doi.org/10.1016/j.agrformet.2012.05.018, 2012.

Horst, T.: A simple formula for attenuation of eddy fluxes measured with first-order-response scalar sensors, 82, 219-233, 1997.

Junninen, H., Ehn, M., Petäjä, T., Luosujärvi, L., Kotiaho, T., Kostiainen, R., Rohner, U., Gonin, M., Fuhrer, K., and Kulmala, M.: A high-resolution mass spectrometer to measure atmospheric ion composition, Atmospheric Measurement Techniques, 3, 1039-1053, 2010.

Kaimal, J. C., Wyngaard, J. C., Izumi, Y., and Coté, O. R.: Spectral characteristics of surface-layer turbulence, Quarterly Journal of the Royal Meteorological Society, 98, 563-589, https://doi.org/10.1002/qj.49709841707, 1972.

Kari, E., Miettinen, P., Yli-Pirilä, P., Virtanen, A., and Faiola, C. L.: PTR-ToF-MS product ion distributions and humidity-dependence of biogenic volatile organic compounds, International Journal of Mass Spectrometry, 430, 87-97, 10.1016/j.ijms.2018.05.003, 2018.

Kim, S., Karl, T., Helmig, D., Daly, R., Rasmussen, R., and Guenther, A.: Measurement of atmospheric sesquiterpenes by proton transfer reaction-mass spectrometry (PTR-MS), Atmos. Meas. Tech., 2, 99-112, 10.5194/amt-2-99-2009, 2009.

Krechmer, J., Lopez-Hilfiker, F., Koss, A., Hutterli, M., Stoermer, C., Deming, B., Kimmel, J., Warneke, C., Holzinger, R., and Jayne, J.: Evaluation of a new reagent-ion source and focusing ion–molecule reactor for use in proton-transfer-reaction mass spectrometry, Analytical chemistry, 90, 12011-12018, 2018.

Striednig, M., Graus, M., Märk, T. D., and Karl, T. G.: InnFLUX–an open-source code for conventional and disjunct eddy covariance analysis of trace gas measurements: an urban test case, Atmospheric Measurement Techniques, 13, 1447-1465, 2020.

Zhao, J. and Zhang, R.: Proton transfer reaction rate constants between hydronium ion (H3O+) and volatile organic compounds, Atmospheric Environment, 38, 2177-2185, https://doi.org/10.1016/j.atmosenv.2004.01.019, 2004.